 DOI: 10.5281/zenodo.3460910

Prototype of a low-cost 3D breast ultrasound imaging system

Vivian Ayres de Souza Luccas
Faculdade de Filosofia, Ciências e Letras de Ribeirão Preto
Universidade de São Paulo
Ribeirão Preto, Brazil
ORCID 0000-0003-2297-1572

Mehran Azimbagirad
Faculdade de Filosofia, Ciências e Letras de Ribeirão Preto
Universidade de São Paulo
Ribeirão Preto, Brazil
ORCID: 0000-0001-6321-7643

Luciana C. Cabrelli
Faculdade de Filosofia, Ciências e Letras de Ribeirão Preto
Universidade de São Paulo
Ribeirão Preto, Brazil
ORCID: 0000-0001-5668-3531

Theo Zeferino Pavan
Faculdade de Filosofia, Ciências e Letras de Ribeirão Preto
Universidade de São Paulo
Ribeirão Preto, Brazil
ORCID 0000-0002-9931-8558

Luiz Otavio Murta Jr.
Faculdade de Filosofia, Ciências e Letras de Ribeirão Preto
Universidade de São Paulo
Ribeirão Preto, Brazil
ORCID: 0000-0002-2197-6008

Antonio Adilton O. Carneiro
Faculdade de Filosofia, Ciências e Letras de Ribeirão Preto
Universidade de São Paulo
Ribeirão Preto, Brazil
ORCID: 0000-0002-1752-7170

***Abstract*— This work describes a setup of the new acquisition system for 3D ultrasound images (i.e. B-mode) for breast tomography. Since premature and precise breast lesions diagnoses turn out in treatment more efficient and save lives, we are looking for a more precise, less painful exams and dose reduction for the patient. Therefore, a low cost scanner mechanism was built aiming to accommodate breasts under water while patient is laid down on a bed in which a robotic arm guides the ultrasound probe to acquire 2D images. Then 3D image is reconstructed using the 2D images due to render the mammary volume searching for lesions. The low cost scanner was built using a regular ultrasound machine, linear probe and major controls made by an Arduino Uno. We compared the acquired phantom images with gold standard images for mammary tissues diagnostics, i.e. Computerized Tomography and Magnetic Resonance Images. This study was evaluated using a paraffin-gel and mineral oil control phantom. Results show that the provided module is convicting enough to be used in local hospital as the next step of this study.**

Keywords—ultrasound, 3D imaging, tomography, Arduino.

I. Introduction

According to *Instituto Nacional de Câncer* (INCA), there will be 59,700 new cases of breast cancer in Brazil over 2018-2019 [1], the first most common cancer [2] for women. If the tumor is diagnosed in early stages, the cure rate is around 95,2%, [3-5] showing the importance of accurate detection method. It is known that the women breast cancer has a higher prevalence then men's most likely reflective of female-related changes in surveillance and/or reproductive risk factors [6-8]. For that reason, women need to take breast scans more often.

Thereat, at age of 40, women start acquiring mammography scans, annually, which uses radiation energy to explore breast tissue looking for tumors or lesions. This kind of exam compresses breast in contact with platforms to enhance image quality [9, 10]. Thus, this exam is considered as painful, turning into quitting of breast test by women [11, 12]. Besides that, there are some studies which correlates radiation doses by mammography scans to breast cancer incidence [13, 14]. Unlike, there are other studies claim that mammography scans aren't enough by itself in diagnosing breast cancer – yet in high fatty density breast or in younger women [15, 16].

As an alternative, ultrasound (US) was introduced. US is a very common exam in clinical routine to diagnostic and characterize breast masses [15-17]. This technique has already been used to complement mammography scans [16] since it has a capability up to 93% sensitivity for detection of mammary masses [18]. Using US is less uncomfortable and brings lower risks for patient [19] in comparison to other imaging techniques.

US is a highly operator dependent skills modality, because requires skillful manipulation of probe, mental ability [20-22], and anatomy knowledge. Because of this, a numerous studies have been focused on developing automatic positioning and probe manipulation aiming to acquire better images quality and precise diagnoses [23-25], as well as 3D image visualization [26, 27].

As an example of 3D US, for breast cancer cases, there are several studies trying to implement these robotic arms or other similar devices looking to develop 3D imaging of mammary tissues [28, 29]. However, all recent provided modalities are using expensive devices and the reconstructed 3D images have artifacts issues. For those cited reasons, this paper describes a new low cost acquisition module for 3D breast imaging which is painless, safer, precise, low budget and has a comparable quality image in respect to computerized tomography (CT) and magnetic resonance image (MRI).

II. Materials and methods

A. Control Phantom

A control phantom was designed aiming to ensure that system measurements and acquisition were correctly performed.

The control phantom was made of paraffin-crystal-gel (8.00 x 8.00 x 7.00 cm^3) with 1% of glass microspheres, providing speckle noise signal and contrast as seen in regular images, and 6.00 ml (± 0.50 ml) mineral oil inclusion (density = 0.87 g/cm^3).

B. Mechanical System

For the mechanical system design, we use a linear probe (L14-5/38 – UltraSonix) which has a physical footprint of 4.00 x 39.00 mm^2. It was attached to a stepper motor (KTC-HT23-401-D 1.80-degree resolution – *Kalatec Automação*) that rotated around its axis. Rotation was performed in steps of 1.44 degrees. Control phantom were placed inside an

 DOI: 10.5281/zenodo.3460910

acrylic cylinder filled with water. Transducer was submerged inside of 10.00 mm of water. Phantom and transducer didn't touch each other. Water was used as coupling source. Probe was attached to the UltraSonix machine to acquire raw data for each step and then processed (see Fig. 1).

Acquisition was performed by this system by edge rotation, i.e., by rotation around the first element. This performed modality gives us a wider view (FOV of 8.00 cm), and requires 360 degrees' acquisition.

Acquisition was using 10MHz, 7.00 cm of depth, and FPS of 15 Mhz.

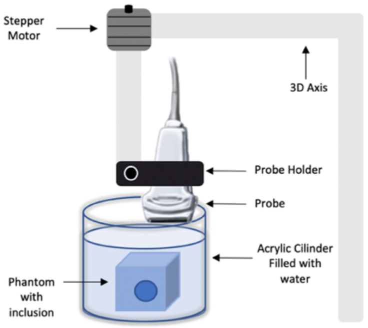

Fig. 1. Scheme of mechanical system.

C. Electronic System

Mechanical system and its rotation needed to be electronically controlled as a fully automatic acquisition. Arduino was chosen as controller, not only because of its good performance in controlling stepper motor but also the low price of the device.

Therefore, the system was controlled by an Arduino Uno (AU) microcontroller. The driver of the AU was coded in C++. The rotation system and US data acquisition was triggered by a TTL pulse (5V pp, 40 ns, 1MHz) from function generator (FG). In order to energize stepper motor, we used a Driver (STR8) and a 40V source.

Schematic design of the 3D acquisition system shown in Fig. 2. Once you press the pushbutton, the system will start the acquisition. AU sends a pulse to the motor, then it will rotate for the angle you settled it for. When the rotation finishes, AU will send another pulse to the function generator, and FG will send a TTL pulse to the Sonix Ultrasound Machine. This process repeats until 360º have been all covered.

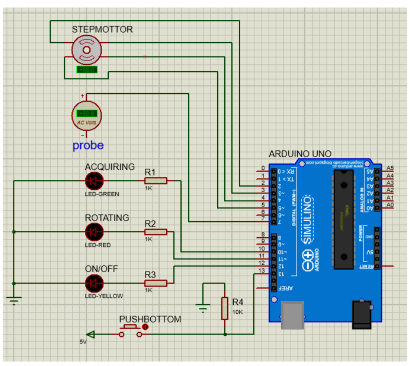

Fig. 2. Acquisition system diagram.

D. Evaluating Imaging Systems:

- MRI:

MRI uses of an assortment of magnetic fields and a resonance that match the radiofrequency of an oscillating magnetic field to the processional frequency of the spin of some hydrogen nucleus in the tissue [30] in order to provide an image.

MRI images were acquired with Phillips Achieva 3.0 T (Philips, EUA), T2, TE = 403.151, TR = 5000, Dimensions = 240 × 240 × 229, Voxel Spacing = 0.67 × 0.67 × 0.70 mm. Image was rendered by 3D Slicer and inclusion was manually segmented from background. Their volume was compared to volume found by needle for the control phantom.

- CT:

Tomography is a modality of image exam which uses produced radiation from bremsstrahlung effect to differentiate between electronic density and establishes contrast. By this, the radiation density is converted in a grey color scale, known as Hounsfield scale [31], and images represent maps of the x-ray attenuation coefficients of the sample.

Tomography images was acquired with a common ear protocol, single beam (120 kVp, 300 mAs), field-per-view of 512 x 512 mm^2, 100 slices spaced by 0.80 mm and gantry inclination of 0º in a Brilliance Big Bore (Philips, EUA) CT scan equipment. Image was rendered by 3D Slicer and inclusion was segmented manually from background. For segmentation, brightness, i.e., Hounsfield scale, were chosen as parameter for delimitation of structures.

III. IMAGE RECONSTRUCTION

A. Pre-processing

A variety of factors can lead to the degradation of the reflected signals, including shadowing due to gas, poor coupling of the transducer, defocusing and attenuation. These effects obscure anatomical details, leading to regions of images with reduced contrast resolution. When it happens, such that boundaries between structures, like the difference between a tumor and the surrounding normal tissue, are undetectable, images are rendered clinically useless.

Furthermore, variability in B-mode images (even when using the same ultrasonic equipment with fixed settings) does exist. For instance, geometrical and diffraction effects, interpatient variation due to depth dependence and inhomogeneous intervening tissue, speckle noise, falsely low echogenicity due to shadowing effects and Low signal-to-noise ratio (SNR) in anechoic components. Many filters as pre-processing steps [32-36] have been introduced since the mentioned artifacts take placed. Respect to which artifacts happen in 3D Ultrasound Image modality, pre analysis of the output image reveals the types of needed filters. Therefore, by modifying the used parameters in the filters, the best performance can be tuned. In this study, we modified an attenuation recovery filter, and after this, we used Envelope filter and then, for correcting the dimension, Mean filter were used.

 DOI: 10.5281/zenodo.3460910

B. Reconstruction

After preparation of image sequences using the filters, let them in a polar system. That means each 2D image will be assumed in a radius R and an angle θ shown in Fig. 3, (a). Let separate all first raw of 2D image sequence. In order to reconstruct the first slice of 3D image which is a planar (Fig. 3, (c)), for each pixel (or voxel in 3D view), there is a distance with the center named x and an angle m. This point can be found approximately on Fig. 3, (b).

To estimate the intensity of point x in 3D volume image, we used a 3×3 the neighbors of x and a 2D interpolation method B-Spline to estimate x intensity level. This approach was used for the second to the last raw.

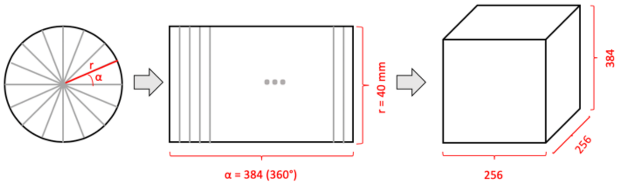

(a) (b) (c)

Fig. 3. Reconstruction strategy for an acquisition protocol. (a) one acquisition protocol by rotation. (b) te first row of all 2D images acquired in step (a). (c) the first slice of 3D image and a voxel x.

IV. Results and Discution

A. Evaluating Imaging Systems:

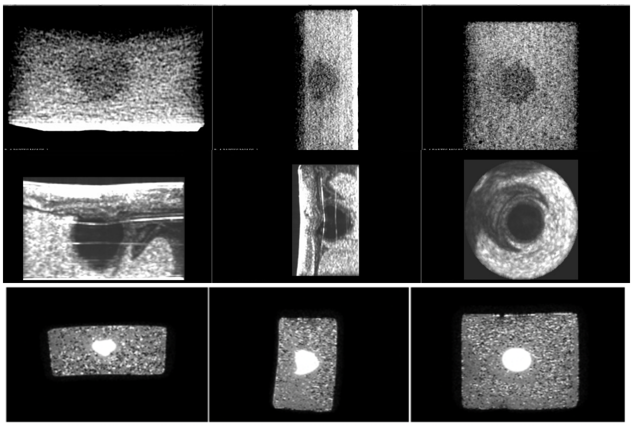

(a) (b) (c)

Fig. 4. Control phantom CT, US images and MRI (T2); (a) Sagittal; (b) coronal (c) axial image view

Images of CT, MRI and US were acquired in order to compare its quality and accuracy for scanning 3D volumes of control phantom (Fig. 4).

For US images, reverberations artefacts can be seen due to the sound reverberation at the bottom of the phantom. Shadows in US images are seem because of mixing the mineral oil inclusion with the background oil-based paraffin-gel.

CT images had low contrast because the inclusion was made of mineral oil and background was oil-based (paraffin-gel) – both with close electronic density.

B. Volume Estimation

The volumes calculated by manual rederization by 3D Slicer software was compared to the volume obtained by volume golden standart images – MRI and CT (Table I).

TABLE I. Volume Estimation

System	Volume (ml)	Accuracy (%)
CT	5.11 ± 0.005	85.17
MRI	6.02 ± 0.005	99.50
US	5.96 ± 0.005	99.33

C. Discussion

Images show an acceptable quality image, with no geometrical artifacts while compounding the images. It has a high accuracy and the images agreed to the MRI as a gold standards images since even 93% is acceptable for correlation between images modalities [37].

Because of the lower contrast of CT, we found a lower accuracy between known volume and the calculated one.

Conclusion

Results have shown the potential of this robotic arm for 3D breast image, considering its high quality imaging and volumetric accuracy. However, because this uses of a regular linear probe, with 4.00 cm footprint, the FOV is restricted to 8.00 cm. The consequence is the limitation of scanned breast size. Using the presented setup only small sizes of breasts (probably to 42C – USA) can be scanned. In conclusion, we present a great 3D ultrasound image with a low-cost equipment, controlled by Arduino Uno. In future works we will improve the system for *in vivo* measurement with data acquisition synchronaized by heart beat or breathing monitor.

Acknowledgment

This paper has no conflict of interest. We would like to thank CNPQ and CAPES for financial support for this work; Prof. Dr. Carlos Ernesto Garrido Salmon for the MRI images; Dr. Alexandre Collelo Bruno for the CT images; Carlos Renato, Agnelo Bastos and Sérgio Bueno for technical support; CSIM laboratory for collaboration and data processing, and GIIMUS laboratory for hosting the studies and experiments.

References

[1] Inca, *Estimativa 2018. Incidência de câncer no Brasil*. 2017, pp. 130-130.

[2] A. C. Society, "Cancer Facts & Figures 2018," *Papermakers Conference, Proceedings of the Technical Association of the Pulp and Paper Industry,* pp. 233-236, 1986.

[3] R. L. Siegel, K. D. Miller, and A. Jemal, "Cancer Statistics, 2017," *CA: a cancer journal for clinicians,* vol. 67, no. 1, pp. 7-30, 2017.

[4] L. Martins Da Rosa and V. Radünz, "Taxa De Sobrevida Na Mulher Com Câncer De Mama: Estudo De Revisão," *Literatura Texto Contexto Enferm Out-Dez,* vol. 21, no. 4, pp. 980-9, 2012.

[5] G. N. Hortobagyi *et al.*, "The global breast cancer burden: Variations in epidemiology and survival," *Clinical Breast Cancer,* vol. 6, no. 5, pp. 391-401, 2005.

[6] I. S. Fentiman, A. Fourquet, and G. N. Hortobagyi, "Male breast cancer," vol. 367, pp. 595-604, 2006.

 DOI: 10.5281/zenodo.3460910

[7] J. R. Weiss, K. B. Moysich, and H. Swede, "Epidemiology of Male Breast Cancer," *Cancer Epidemiology, Biomarkers & Prevention,* vol. 14, no. January, pp. 20-27, 2005.

[8] W. F. Anderson, M. D. Althuis, L. A. Brinton, and S. S. Devesa, "Is male breast cancer similar or different than female breast cancer ?," *Breast Cancer Research and Treatment,* no. 1, pp. 77-86, 2004.

[9] S. d. P. Bauab, "Mamografia digital: um caminho sem volta," *Radiologia Brasileira,* vol. 38, no. 3, pp. iii-iv, 2005.

[10] M. Heath *et al.*, "Current Status of the Digital Database for Screening Mammography," *Springer Science+Business Media,* pp. 457-460, 1998.

[11] R. F. Júnior, W. F. Fiori, F. J. d. F. Ramos, E. Godinho, and R. M. S. Rahal, "Desconforto e dor durante realização da mamografia," *Revista Associação Médica Brasileira,* vol. 52, no. 5, pp. 333-336, 2006.

[12] A. Are, T. Eerola, and M. Pamilo, "Pain and Discomfort During Mammography," vol. 32, no. 10, pp. 1674-1679, 1996.

[13] M. e. Al, "Benefits versus Risks from Mammography," *Department of Radiology, University of New Mexico,* vol. 79, no. 3, pp. 903-909, 1997.

[14] R. E. Hendrick, "Radiation Doses and Cancer Risks from Breast Imaging Studies," *Radiology,* vol. 257, no. 1, pp. 246-253, 2010.

[15] F. Gharekhanloo, M. M. Haseli, and S. Torabian, "Value of ultrasound in the detection of benign and malignant breast diseases: A diagnostic accuracy study," *Oman Medical Journal,* vol. 33, no. 5, pp. 380-386, 2018.

[16] C. M. C. P. R. S. G. R. B. F. E. R. D. G.-S. F. W. B. G. Kenneth J. W. Taylor and M. Ellen, "Ultrasound as a complement to mammographyand breast examination to characterize breast masses," *Ultrasound in Medicine & Biology,* vol. 28, no. 1, pp. 36-39, 2002.

[17] A. Itoh *et al.*, "Breast Disease: Clinical Application of US Elastography for Diagnosis," *Radiology,* vol. 239, no. 2, pp. 341-350, 2006.

[18] D. Lister *et al.*, "The accuracy of breast ultrasound in the evaluation of clinically benign discrete, symptomatic breast lumps," *Clinical Radiology,* 1998.

[19] T. Effects, "Biological Effects of Diagnostic Ultrasound: A Review 1," no. October 1977, pp. 479-483, 1978.

[20] P. Chevallier *et al.*, "Influence of operator experience on performance of ultrasound-guided percutaneous liver biopsy," *European Radiology,* vol. 14, no. 11, pp. 2086-2091, 2004.

[21] M. A. M. D. Oyley, J. E. C. B. Amber, F. R. F. Uechsel, and N. I. L. B. Ush, "A freehand elastographic imaging approach for clinical breat imaging: System development and perfomance evaluation," *Ultrasound in Medicine & BiologyMedicine,* vol. 27, no. 10, pp. 1347-1357, 2001.

[22] E. Miller, "Hand-Held Sonography Breast," *AJR,* pp. 623-627, 1985.

[23] P. A. Patlan-Rosales and A. Krupa, "A robotic control framework for 3-D quantitative ultrasound elastography," *Proceedings - IEEE International Conference on Robotics and Automation,* pp. 3805-3810, 2017.

[24] P. M. Loschak, L. J. Brattain, and R. D. Howe, "Automated pointing of cardiac imaging catheters," *Proceedings - IEEE International Conference on Robotics and Automation,* pp. 5794-5799, 2013.

[25] F. Ernst, "Robots take ultrasound to the fourth dimension," *Research features,* pp. 37-38.

[26] M. R. Morgan, J. S. Broder, J. J. Dahl, and C. D. Herickhoff, "Versatile Low-cost Volumetric 3D Ultrasound Platform for Existing Clinical 2D Systems," *IEEE Transactions on Medical Imaging,* vol. 37, no. 10, pp. 2248-2256, 2018.

[27] L. J. Brattain, P. M. Loschak, C. M. Tschabrunn, E. Anter, and R. D. Howe, "Instrument Tracking and Visualization for Ultrasound Catheter Guided Procedures," *Augmented Environments for Computer-Assisted Interventions,* pp. 41-50.

[28] J. A. Shipley *et al.*, "Automated quantitative volumetric breast ultrasound data-acquisition system," *Ultrasound in Medicine and Biology,* 2005.

[29] B. Treepong, N. Tanaiutchawoot, C. Wiratkapun, and J. Suthakorn, "On the design and development of a breast biopsy navigation system: Path generation algorithm and system with its GUI evaluation," *2014 IEEE-EMBS International Conference on Biomedical and Health Informatics, BHI 2014,* pp. 273-276, 2014.

[30] R. W. Brown, Y.-C. N. Cheng, E. M. Haacke, M. R. Thompson, and R. Venkatesan, *Magnetic Resonance Imaging - Physical Principles and Sequence Design*, Second Edi ed. Wiley Blackwell, 2014, pp. 1-978.

[31] R. K. Hobbie and B. J. Roth, *Intermediate Physics for Medicine and Biology*, 4th editio ed. Springer International Publishing, 2007.

[32] M. Azimbagirad, A. Carlos, S. Filho, A. Carlos, L. Otavio, and M. Junior, "Partial volume transfer (PVT) conversion of cerebral tissue volumes between different magnetic fields MRI," *Research on Biomedical Engineering,* 2019.

[33] F. Natterer and F. Wubbeling, "A propagation-backpropagation method for ultrasound tomography," *Inverse Problems,* vol. 11, no. 6, pp. 1225-1232, 1995.

[34] J. F. Krucker, C. R. Meyer, G. L. LeCarpentier, J. B. Fowlkes, and P. L. Carson, "3D spatial compounding of ultrasound images using image-based nonrigid registration," *Ultrasound Med Biol.,* vol. 26, no. 9, pp. 1475-1488, 2000.

[35] R. N. Rohling, A. H. Gee, and L. Berman, "Automatic registration of 3-D ultrasound images," *Ultrasound in Medicine and Biology,* vol. 24, no. 6, pp. 841-854, 1998.

[36] G. Xiao, J. M. Brady, J. A. Noble, M. Burcher, and R. English, "Nonrigid registration of 3-D free-hand ultrasound images of the breast," *IEEE Transactions on Medical Imaging,* vol. 21, no. 4, pp. 405-412, 2002.

[37] K. M. Pohl *et al.*, "A hierarchical algorithm for MR brain image panellation," *IEEE Transactions on Medical Imaging,* vol. 26, no. 9, pp. 1201-1212, 2007.